

Influence of the cross-section shape in the capillaries on the wetting properties demonstrated by the calculated wetting angles

K.H. Hartge*, J. Bachmann and S.K. Woche

Institute of Soil Science, University of Hannover, Herrenhaeuser Str. 2, 30419 Hannover, Germany

Received June 2, 2003; accepted September 15, 2003

A b s t r a c t. Earlier results had shown that the contracting force of water films between parallel solid surfaces increased when they were deformed to give longer menisci by subdividing the water volume. Since deformations of this kind will occur regularly when soils are tilled or wheeled with machinery the question was raised how such events would change soil capillary properties. Circular capillaries with a concave inner surface were compared to the ones with a convex inner surface. They were formed by the fixing of either three or four rods with circular diameter together. Perimeters and cross-sectional areas were calculated and the height of capillary rise was measured by two independent methods. For comparison, the results of wetting angles were used. They were calculated from an average inner diameter of the capillaries and separately measured using the height of menisci. The present results showed that in the convex capillaries, higher angles were calculated in comparison to those independently measured at the outsides of rods and tubes. The angles calculated from the capillary height measured in the circular capillaries were smaller than those measured at the outside of the tubes. It was concluded that the wetting angles measured directly with an optical equipment were affected by the solid phase geometry. The above result emphasized that contact angles resulted from a combination of several distinct factors. The curvature of the contact line is one of them.

K e y w o r d s: capillary rise, capillary cross section, wetting angles

INTRODUCTION

Since Buckingham (1907) developed a theory for describing water potential in unsaturated soils, a great number of investigations were conducted in this field (van Genuchten, 1980; Raats, 2001; Bachmann and van der Ploeg, 2002). To relate that water potential with pore geometry of the soil, a well known equation for the capillary rise in a circular tube was used (Eq. (1)):

$$h = 2 \gamma \cos \alpha / (r d g), \quad (1)$$

where: h is height (cm), γ is liquid surface tension (g s^{-2}), α is a liquid-solid wetting angle ($^\circ$), r is a radius of the capillary (cm), d is liquid density (g cm^{-3}), and g is gravitation (cm s^{-2}). In soils, there are generally capillaries different from pores with a circular shape. Moreover, pores are deformed by strains which are exerted by trafficking or by tillage treatment. These processes are measurable down to the subsoil (Horn and Hartge, 2001). It has been hypothesized that such deformations of either menisci or pore shapes will influence capillary phenomena in the cases where the perimeter-shape of the capillaries is definitely other than circular.

Earlier investigations of Hartge and Bachmann (2000) showed that a contracting force that was developed by menisci between two parallel orientated plates is not determined merely by the plates distance, a total water volume and an average area of water/solid interface. It was clearly shown that subdividing the water volume from one single meniscus into several smaller ones increased the contracting force. Since the total meniscus length was the only difference between the two experiments, it was concluded that the length of the three phase contact line can be identified as an additional factor for the contracting force caused by the water drops. Beside that effect, the objective of the present study was to identify the impact of the pore geometry on the capillary rise.

MATERIAL AND METHODS

For the use of Eq. (1), it is implicitly assumed that a capillary is cylindrical in shape. If this equation is expanded

*Corresponding author's e-mail: k.hartge@arcor.de

to include an explicitly circular cross section it can be written as:

$$F h d g = U g \cos \alpha, \quad (2)$$

where: F (cm^2) is the area of the cross section ($F = r^2 \pi$) and U (cm) is the circumference with $U = 2\pi r$. The numerical values used for calculations were $\gamma = 73.2 \text{ g s}^{-2}$, for $d = 0.998 \text{ g cm}^{-3}$ and for $g = 981 \text{ cm s}^{-2}$.

To produce capillary tubes with various cross-sectional shapes, circular glass rods were used with diameters of 3, 6 and 10 mm. These rods were fixed together to give bundles of three or four parallel fixed rods, respectively. Accordingly, the centres of the circular cross sections of the rods formed either as a triangle or a square (Fig. 1).

A capillary between the three rods then had a perimetric shape of a triangle with the sides bent inwardly. A capillary between the four rods formed likewise a square with the sides bent inwardly. These capillaries were called convex ones (Table 1). For comparison, laboratory capillary tubes were used with radii of 0.058 and 0.15 cm. These capillaries were termed as concave ones.

Cross sections and perimeters of the laboratory capillaries were calculated using the Eqs (3)-(7). For a 4-rod capillary (Fig. 1) the perimeter was calculated with:

$$U_4 = 2 \pi r_r, \quad (3)$$

where: r_r is the radius of the rod. Cross section of 4-rod capillaries was calculated according to:

$$F_4 = (2 r_r)^2 - r_r^2 \pi. \quad (4)$$

For 3-rod capillaries (see Fig. 1) the perimeters were calculated using:

$$U_3 = \pi r_r. \quad (5)$$

Their cross section was calculated with:

$$F_3 = \sin \alpha 2 r_r^2 - r_r^2 \pi / 2. \quad (6)$$

Furthermore, the radii of circular capillaries formed inside of the 3- and 4-rod combinations were calculated:

$$\text{a 3-rod -capillary: } r_{\text{inside}} = r_{\text{rod}} / \cos 30^\circ - r_{\text{rod}} \quad (7)$$

$$\text{a 4-rod -capillary: } r_{\text{inside}} = r_{\text{rod}} / \sin 45^\circ - r_{\text{rod}} .$$

Perimeters and cross-sections of all capillaries, i.e., normal circular, 3-rod and 4-rod, are presented in Table 1.

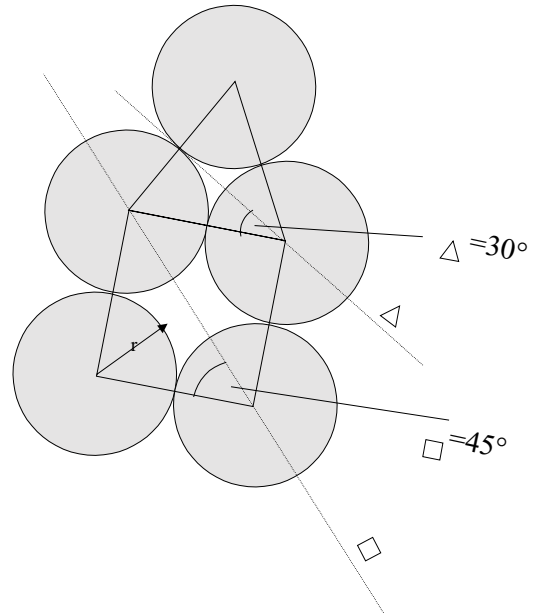


Fig. 1. Schema of three-rod and four-rod capillaries with convex solid surfaces. Line of sighting for measurement dotted.

Table 1. Cross-section (F), perimeter (U), their ratios (U/F , F/U) for rod-capillaries (3-rod, 4-rod) and for circular capillaries

Capillary (cm)	F (cm^2)	U (cm)	U/F	F/U
Three-rod capillary				
$r_{\text{rod}} = 0.15$	0.0036	0.472	131.1	0.0076
$r_{\text{rod}} = 0.30$	0.0145	0.942	64.9	0.0154
$r_{\text{rod}} = 0.50$	0.0403	1.570	38.9	0.0257
Four-rod capillary				
$r_{\text{rod}} = 0.15$	0.0193	0.942	48.8	0.0205
$r_{\text{rod}} = 0.30$	0.0772	1.880	24.3	0.0411
$r_{\text{rod}} = 0.50$	0.2146	3.140	14.6	0.0684
Circular tublets				
$r = 0.058$	0.0105	0.364	34.5	0.0289
$r = 0.10$	0.0314	0.628	20.0	0.0500
$r = 0.15$	0.0707	0.942	13.3	0.0752

Measurements of the capillary rise were conducted using the device as shown in Fig. 2.

A mm-scale and a cuvette (a glass vessel) with plane walls were fixed on a tripod which was adjustable in a vertical direction. For the measurement, the capillary was positioned in the cuvette. Rising and lowering water level in the cuvette made it possible to observe menisci at the advancing and retreating state and to repeat measurements at different positions in the capillaries. Readings were taken to an accuracy of 0.1 mm from a fixed position independent of the movable tripod. This procedure was denominated as an ‘accurate method’.

Because of the two plane walls of the cuvette and particularly because of the optical effect of the glass rods associated with the problem to identify the meniscus height within the bundle of rods accurately (a lens-like refraction of light within the glass rods), we had some doubts as to the reliability of the menisci-readings. Therefore a second method was used. It consisted in the preparation of separate specimens with 5 cm length of all rod combinations and submerging the bundles completely in the liquid causing the pore space to fill completely with water. Thereafter the bundles were pulled completely out of the liquid and held vertically until the last droplet of water fell. Then the capillary was positioned horizontally and the length of the water column was measured to an accuracy of 1 mm. When using the above procedure water menisci were exactly visible. The disadvantage of this method was that the length of the water column varied depending on the size of the last falling droplet after lifting out of the water (Hartge, 1998). With this procedure draining situations according to receding water

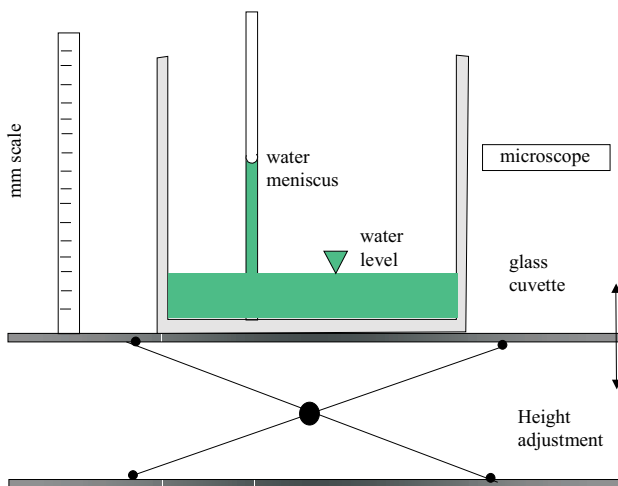


Fig. 2. Experimental device. Reference-vessel (cuvette), capillary and mm-scale movable on a tripod. Change of the meniscus height in the capillary due to the lifting (the advancing situation) and lowering (the retreating situation) out of the water level in the cuvette.

menisci were obtained. This procedure was denominated as a ‘makeshift method’.

Angles of wetting angles with water from all rods and capillary tubes were measured directly using a special microscope with a goniometer (Bachmann, 1988). Values of the circular capillaries were also taken at the outside of the tubes. This additional measurement allows for the direct comparison of easily readable contact angles on either convex (an inner wall of the circular capillary) or concave shaped surfaces (an outer wall of the circular capillary and a round rod surface).

Before each series of measurements, glass capillaries and glass rods were cleaned using a mixture of CrVI with H₂SO₄. All measurements were taken using deionised water.

RESULTS

Values of the capillary rise measured with the accurate method (Fig. 2) are given in Table 2.

As expected, the capillary ascent measured for the advancing situation were lower than for the retreating situations. The results of the makeshift method are given in Table 3. They correspond generally to the retreating situations.

This specific mode is considered as the main reason for the variations which are greater than those obtained with the accurate method. However, the results of both methods show a close correlation. The regression of both is given by:

$$y = -0.38 + 1.27 x, \quad (8)$$

with x as accurate values and y as values measured with the makeshift method. The coefficient of correlation is $r = 0.947$ at 8 pairs of observation ($DF = 6$) and is characterized by the significance level of $p < 0.1\%$ (Sachs, 1978). Since standard deviations with the accurate method were smaller than those with the makeshift method, the values of the first one was used for further discussion.

In order to assess the impact of the capillary cross section shape (either convex or concave) a reference is needed. For this issue the wetting angle α or its cosine can be chosen. It is the only term in Eq. (2) which can neither be obtained from the measurements inside various capillaries nor taken from standard tables of physical constants and properties. For the rod-capillaries the values for U and F were taken from Table 2. For heights h of capillary rise the measured values were taken. The results calculated after rearranging Eq. (2) to Eq. (9):

$$\cos \alpha = F h d g / (U \gamma) \quad (9)$$

are shown in Table 4. Independently measured wetting angles at the rods and tubes were also summarised.

As can be seen, the wetting angles which were measured directly at the surfaces do not fit with the calculated ones,

Table 2. Arithmetic mean, standard deviation, median, and number of measurements for the accurate method

Capillary (mm)		Arithmetic mean (cm)	Standard deviation (cm)	Median (cm)	n
Advancing state					
3 rod	1.5	3.30	0.135	3.31	6
	3.0	2.23	0.108	2.26	4
	5.0	1.26	0.096	1.27	4
4 rod	1.5	1.54	0.061	1.54	4
	3.0	0.79	0.066	0.78	6
	5.0	0.34	0.023	0.33	4
Circular	0.58	2.47	0.053	2.50	9
	1.50	0.93	0.014	0.93	7
Receding state					
3 rod	1.5	3.50	0.110	3.51	9
	3.0	2.47	0.054	2.48	6
	5.0	1.40	0.011	1.40	6
4 rod	1.5	1.84	0.075	1.80	6
	3.0	0.91	0.073	0.90	9
	5.0	0.40	0.015	0.40	6
Circular	0.58	2.50	0.031	2.49	9
	1.50	0.94	0.013	0.94	7

Table 3. Length of water-columns in capillaries after lifting out of the water (the makeshift method) 10 replications (a receding wetting front)

Capillary type		Mean (cm)	Standard deviation (cm)
3 rod	0.15	4.22	0.42
	0.30	1.95	0.15
	0.50	0.92	0.06
4 rod	0.15	2.14	1.11
	0.30	0.86	0.05
	0.50	0.20	n.o.*
Circular	0.058	0.99	0.15
	0.15	3.40	0.12

*At the moment of lifting out of the water, menisci broke. Therefore no standard deviation could be calculated. The mean is an estimation.

e.g., for the 3- and 4 rod-capillaries higher angles were calculated than those measured separately at the outsides of the rods. On the other hand, for the circular capillary tubes, the values which were calculated in the classical way for the inner surfaces were smaller than those directly measured at their outer surface.

DISCUSSION

Table 4 shows that the separately measured wetting angles of all rods and tubes (columns 5 and 6) are rather

similar, e.g., the differences between them are not significant. Thus wetting properties of these materials can be considered as the same.

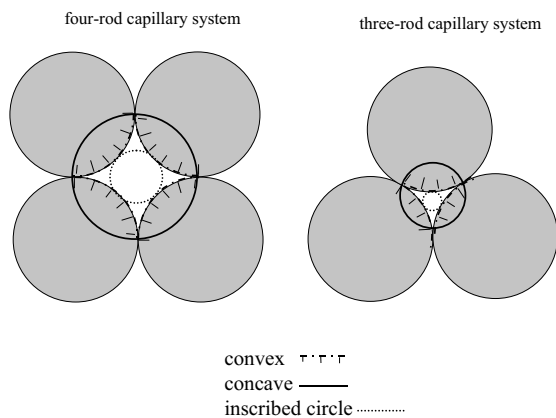
The calculated wetting angles inside the convex rod capillaries are greater than the measured ones, whereas the calculated wetting angles inside the concave circular ones are smaller (columns 3 and 4). In order to assess these differences, the angles were calculated for virtual circular capillaries constructed into the rod-capillaries as indicated by Fig. 3. This calculation gave values between $\cos \alpha = 0.99604$ and 0.99991 . In this case, as expected, wetting angles close to zero were obtained (Table 4, column 7). From this result it is assumed, that the different wetting angle values in the other columns are quite substantial.

The wetting angles in Table 4 can be subdivided into the values obtained using the measured menisci heights (columns 3, 4) and the wetting angles measured directly (columns 5, 6). The first group consists of the values calculated either from convex cross-sections (a bundle of rods) or concave capillaries as was the case with circular capillaries. The second group however, includes only the values obtained from the measurements taken at convex surfaces of the solid material, e.g., from the rods immersed partially in water and outsides of circular capillaries. This fact means that the actual angle of wetting is influenced by differences in the wetting energy that is brought about by the different cross-sections geometry which is compensated by the value of $\cos \alpha$ in Eq. (7). Then the most obvious difference is the direction of bending of the solid surfaces relative to the liquid contact line.

Table 4. Wetting angles ($^{\circ}$) calculated with Eq. (7), measured capillary height and inner capillaries calculated for the equivalent (see Fig. 3)

Capillary type		Wetting angles ($^{\circ}$)				
		Calc. Eq. (7)	Group mean	Measured	Group mean	Equivalent cap.
3 rod	0.15	68.4	62.8	39.0 ± 4.2	39.0	5.1
	0.30	59.0		40.7 ± 2.2		2.3
	0.50	61.2		37.3 ± 2.2		3.8
4 rod	0.15	60.4	63.0	39.0 ± 4.2	39.0	4.9
	0.30	60.3		40.7 ± 2.2		4.0
	0.50	68.5		37.3 ± 2.2		3.9
Circular		Inside		Outside		
	0.058	16.3	18.5	46.9 ± 3.0	41.4	n.o.
	0.10	n.o.*		n.o.*		n.o.
	0.15	20.7		35.9 ± 7.5		n.o.

*n.o. - no observation.

**Fig. 3.** Relation of geometry of convex, concave and inscribed circular pores.

CONCLUSIONS

These results suggest that macroscopic, i.e., phenomenologically observable wetting angles are not merely dependent on the well known variables like intrinsic interfacial energy in the way described in Eq. (1) and, consequently, Eq. (2) and (9) derived from the former. This means that the models used here created situations beyond the applicability of the original equation. One variable which under the chosen conditions influences the macroscopically observed wetting angle is the curvature of the solid surface in the right-angled (orthogonal) position to the wetting fluid.

Thus from the results obtained, it can be concluded, that the conditions of wetting in the porous media made up from grains of different shape are beyond the applicability range of these equations as well.

This fact severely narrows the value of data of the equivalent pore diameters calculated in the usual way.

Strictly speaking, all results presented here would apply only to glass or pure quartz sand and water. In soils, however, mineral surfaces are more or less completely covered by organic films and solid organic particles can make up part of the material. Soil solution is not pure water either but contains organic and inorganic components which influence surface energy. Furthermore, earlier results showed that phenomenologic wetting angles were strongly effected by the mechanical working of the samples, i.e., the changing of the relative particles positions by the destroying of aggregation (Ellies *et al.*, 2003).

These observations and explanations fit well with the general concept as given in the standard literature (Adamson, 1990, p. 46). However, these findings are not part of the standard soil physics literature. The importance of the soil specific wettability indicated by systematic differences between the values of the Sessile Drop Method and the Wilhelmy Plate Method (Bachmann *et al.*, 2001) pointed into the same direction. Obviously, the wetting angles measured directly with liquids at glass surfaces or other solid material surfaces should only be compared if the solid surface has an equal shape, say plane or bent in same direction. This makes us conscious of the fact that a wetting angle is not a consistent physical property, but the result of combinations of several factors, one of them being the geometry of the solid surface.

REFERENCES

- Adamson A.W., 1999.** Physical Chemistry of Surfaces. 5. Ed. J.Wiley and Sons, New York.
- Bachmann J., 1988.** Impact of Organic Substance with Different Degrees of Humification on Soil Physical Properties (in German) Diss. Univ. Hannover, Dept. of Earth Sciences.

- Bachmann J., Woche S. K., Goebel O.M., and Fischer W. R., 2001.** Contact Angle and Surface Charge of Various Mixtures of Wetttable and Hydrophobic Silt Particles. *Rev. Ciencia del Suelo y Nutr. Veg.*, 1, 26-33.
- Bachmann J. and van der Ploeg R.R., 2002.** A review on recent developments in soil water retention Theory: Interfacial Tension and Temperature Effects. *J.Plant Nutr. Soil Sci.*, 165, 468-478.
- Buckingham E., 1907.** Studies on the movement of soil moisture. USDA-Bureau of Soils Bull., 38. Washington, D.C.
- Ellies A., Hartge K.H., MacDonald R., and Ramirez C., 2003.** Organic matter and wetting properties of soil samples - an interpretation. *J.Plant Nutr. Soil Sci.*, 166, 120-123.
- Hartge K.H., 1998.** Faktoren für die Wirksamkeit einer Kapillarsperre. *Z.Kult. und Landentw.*, 39, 194-198.
- Hartge K.H. and Bachmann J., 2000.** The capillary action of water as a function of meniscus length and wetting angle. *Soil Sci.*, 165, 759-767.
- Horn R. and Hartge K.H., 2001.** Das Befahren von Ackerflächen als Eingriff in den Bodenwasserhaushalt. *Wasser and Boden*, 53, 9-11.
- Raats P.A.C., 2001.** Developments in soil-water physics. *Geoderma, Special Issue*, 100(3-4), 355-387.
- Sachs L., 1978.** *Angewandte Statistik*. 5. Aufl. Springer, Berlin/Heidelberg.
- Van Genuchten M.Th., 1980.** A closed-form equation for predicting the hydraulic conductivity of unsaturated soils. *Soil Sci. Soc. Amer. J.*, 44, 892-898.